A comparison of visual responses in the lateral geniculate nucleus of alert and anaesthetized macaque monkeys

Henry J. Alitto[1], Bartlett D. Moore 4th[1], Daniel L. Rathbun[1] and W. Martin Usrey[1,2,3]

[1] *Center for Neuroscience, University of California – Davis, Davis, CA 95618, USA*
[2] *Department of Neurobiology, Physiology and Behavior, University of California – Davis, Davis, CA 95618, USA*
[3] *Department of Neurology, University of California – Davis, Sacramento, CA 95817, USA*

Non-technical summary Neurons in the lateral geniculate nucleus (LGN) of the thalamus are the major source of visual input to the cerebral cortex. Much of our understanding of the physiology of LGN neurons comes from data collected in anaesthetized animals. This study examines the visual responses of LGN neurons in alert animals and compares these responses to those from anaesthetized animals. Compared to the anaesthetized animal, LGN neurons in the alert animal respond to visual stimuli with stronger responses and follow stimuli drifting at higher spatial and temporal frequencies. Stronger responses are likely to translate into an increased coupling between the LGN and visual cortex, as firing rate and interspike interval are known to influence the dynamics of synaptic communication between the two structures.

Abstract Despite the increasing use of alert animals for studies aimed at understanding visual processing in the cerebral cortex, relatively little attention has been focused on quantifying the response properties of neurons that provide input to the cortex. Here, we examine the response properties of neurons in the lateral geniculate nucleus (LGN) of the thalamus in the alert macaque monkey and compare these responses to those in the anaesthetized animal. Compared to the anaesthetized animal, we show that magnocellular and parvocellular neurons in the alert animal respond to visual stimuli with significantly higher firing rates. This increase in responsiveness is not accompanied by a change in the shape of neuronal contrast response functions or the strength of centre–surround antagonism; however, it is accompanied by an increased ability of neurons to follow stimuli drifting at higher spatial and temporal frequencies.

(Received 25 March 2010; accepted after revision 1 July 2010; first published online 5 July 2010)
Corresponding author W. M. Usrey: Center for Neuroscience, University of California, Davis, CA 95618, USA. Email: wmusrey@ucdavis.edu

DOI: 10.1113/jphysiol.2010.190538

Introduction

Neurons in the lateral geniculate nucleus (LGN) of the thalamus are the primary source of visual input to the cerebral cortex. In primates, LGN neurons are segregated into magnocellular, parvocellular and koniocellular layers. Based on studies performed largely on anaesthetized animals, we have obtained a tremendous understanding of the visual physiology of LGN neurons. Notably, magnocellular neurons respond better to low contrast stimuli and follow stimuli at higher temporal frequencies than parvocellular neurons (Kaplan & Shapley, 1982, 1986; Hicks *et al.* 1983; Derrington & Lennie, 1984; Derrington *et al.* 1984; Norton *et al.* 1988; Benardete *et al.* 1992; Spear *et al.* 1994; O'Keefe *et al.* 1998; Solomon *et al.* 1999; Usrey & Reid, 2000; Levitt *et al.* 2001; Movshon *et al.* 2005; but see Spear *et al.* 1994; Hawken *et al.* 1996). However, with the increasing use of alert primates in studies examining visual processing in primary visual cortex and beyond, it is important to re-evaluate the physiology of LGN neurons in the alert animal. In so doing, we can gain a better understanding of how visual inputs to the cortex underlie cortical activity and visual behaviour.

Although it is generally assumed that the major differences between magnocellular and parvocellular neurons reported for anaesthetized animals should hold for alert animals, the details of these differences may be affected by anaesthesia. For instance, common agents used for anaesthesia, such as isoflurane, urethane, pentothal, nembutal, sufentanil and propofol, are known to have a variety of effects on synaptic transmission and/or neuronal excitability (Paddleford, 1999; Dilger, 2002; Campagna *et al.* 2003; Rudolph & Antkowiak, 2004; Evers & Crowder, 2005). Consequently, visual responses in the LGN of alert animals may be significantly stronger than those in the anaesthetized animal. Along these lines, an increase in neuronal excitability could be accompanied by shifts in tuning functions, response reliability, and/or the balance of centre–surround antagonism.

This study provides a quantitative examination of visual responses in the LGN of alert macaque monkeys. Data are also provided for comparison from macaque monkeys anaesthetized with a combination of sufentanil citrate ($6\ \mu g\ kg^{-1}\ h^{-1}$) and isoflurane (0.4%). For both magnocellular and parvocellular neurons, our results show that response reliability, centre–surround antagonism and the shape of neuronal contrast response functions are similar for neurons in the alert and anaesthetized animal. In contrast, magnocellular and parvocellular neurons in the alert animal respond to visual stimuli with significantly higher firing rates and follow stimuli drifting at significantly higher temporal frequencies. Magnocellular neurons in the alert animal also follow stimuli at significantly higher spatial frequencies.

Methods

Single-unit recordings were made from LGN neurons in two alert and 10 anaesthetized macaque monkeys (*Macaca mulatta*). For both alert and anaesthetized animals, receptive fields were parafoveal (>90% within the central 20 deg). Data from a subset of neurons also contributed to a recent study examining the temporal dynamics of extraclassical suppression in the primate (Alitto & Usrey, 2008). This study used contrast response functions to classify magnocellular and parvocellular neurons; it did not examine maximum or spontaneous firing rates, temporal frequency tuning, spatial frequency tuning, centre–surround interactions, response reliability, or burst activity in the alert or anaesthetized animal.

Surgery and preparation

All surgical and experimental procedures conformed to NIH guidelines, were in accordance with the policies and regulations described in this journal (Drummond, 2009), and were carried out with the approval of the Animal Care and Use Committee at the University of California, Davis.

For experiments in anaesthetized animals, anaesthesia was induced with ketamine ($10\ mg\ kg^{-1}$, I.M.) and maintained with sufentanil citrate ($6\ \mu g\ kg^{-1}\ h^{-1}$, I.V.) and isoflurane (0.4%). Animals were placed in a stereotaxic apparatus where the temperature, electrocardiogram, electroencephalogram and expired CO_2 were monitored continuously. Proper anaesthetic depth was assessed by monitoring the EEG for changes in slow-wave or spindle activity and the ECG and expired CO_2. If changes in any of these measures indicated a decreased level of anaesthesia, additional sufentanil was given and the rate of infusion increased. Pupils were dilated with 1% atropine sulfate and eyes were glued to posts attached to the stereotaxic frame. The eyes were fitted with contact lenses and focused on a tangent screen located 172 cm in front of the animal. A midline scalp incision was made and wound margins were infused with lidocaine. A small craniotomy was made above the LGN. Once all surgical procedures were complete, animals were subjected to neuromuscular block with vecuronium bromide ($0.2\ mg\ kg^{-1}\ h^{-1}$, I.V.) and mechanically respired. At the end of each experiment, animals were killed with an overdose of sodium pentobarbital ($100\ mg\ kg^{-1}$, I.V.).

Under full surgical anaesthesia (isoflurane 1.5–2.0%), the animals used for alert recordings were equipped with a scleral eye coil and a cranial implant containing a head restraint post and a recording cylinder.

Data acquisition and visual stimuli

Single-unit responses from LGN neurons were made using platinum-in-glass electrodes (Alpha Omega, Nazareth

Illit, Israel). Responses were amplified, filtered and recorded to a PC with a Power 1401 data acquisition interface and Spike 2 software (Cambridge Electronic Design, Cambridge, UK). Visual stimuli were created with a VSG2/5 (Cambridge Research Systems, Rochester, UK) and presented on a gamma-calibrated Sony monitor running at 140 Hz. The mean luminance of the monitor was 38 candelas m^{-2}.

Visual responses of LGN neurons were characterized quantitatively using drifting sinusoidal gratings (vertical orientation). For experiments with anaesthetized animals, drifting gratings were shown for 4 s, followed by 4 s of mean grey. For experiments with alert animals, drifting gratings were shown for 3 s while animals maintained fixation for a fluid reward. Proper fixation was the only behavioural task required for the reward. Trials were immediately aborted if eye position, measured with a scleral eye coil, deviated by more than 0.35 deg. The inter-stimulus interval was >3 s and the screen was mean grey. For both anaesthetized and alert recordings, the size of the visual stimulus was ∼3 times the size of the classical receptive field. Importantly, with the exception of stimulus duration, all comparisons of neuronal responses between alert and anaesthetized animals were made using identical stimuli (e.g. stimulus size, contrast and temporal frequency).

Spatial frequency tuning

Spatial frequency tuning curves were made both to determine the optimal spatial frequency for subsequent grating experiments and to assess the spatial frequency to evoke a response 50% of maximum (SF_{50}), and the strength of the receptive field surround, relative to the centre. Responses to drifting sine-wave gratings (4 Hz, 100% contrast) presented at 10–16 different spatial frequencies (typical range: 0.1 to 10 cycles deg^{-1}) were fitted to a frequency domain difference of Gaussians (DOG_F) equation,

$$R(f) = K_c \exp(-(\pi r_c f)^2) - (K_s) \exp(-1(\pi r_s f)^2)$$

where $R(f)$ is the first harmonic (f_1) of the response evoked by spatial frequency f, r_c is the radius of the centre subunit, and r_s is the radius of the surround subunit. A constrained non-linear optimization procedure (MATLAB function: fmincon; The Mathworks Inc., Natick, MA, USA) was used to minimize the squared error (i.e. Σ (Data-Fit)^2) when fitting the DOG_F functions and all subsequent data sets.

To examine the relative strength of surround antagonism, we calculated an antagonism index:

$$\text{Antagonism Index} = 1 - \text{Response (low spatial freq.)} / \text{Response (preferred spatial freq.)}$$

With this equation, a neuron with equal response rates to the lowest spatial frequency examined and the preferred spatial frequency would have an antagonism index of zero, while a neuron with no response to the lowest spatial frequency would have an index equal to 1.

Contrast response functions

To determine the influence of contrast on neuronal activity, contrast response functions were made from responses (first harmonic, f_1) to drifting sine-wave gratings (4 Hz, preferred spatial frequency) presented over a range of contrasts (0.1% to 100%). Neuronal responses were fitted to a hyperbolic ratio (Albrecht & Hamilton, 1982):

$$R(C) = K(C^n/(C^n + C_{50}^n)) + DC$$

where C represents the contrast levels presented during the experiment, K represents the maximum response (f_1), C_{50} is the contrast corresponding to 50% of the cell's maximum response, DC is the firing rate to a blank grey screen, and n is a variable reflecting the cell's sensitivity.

Temporal-frequency tuning

Temporal-frequency tuning curves were made from neuronal responses (first harmonic, f_1) to drifting sinusoidal gratings (0.5 to 64 Hz; 100% contrast; preferred spatial frequency). Response curves were interpolated with a cubic spline to determine the preferred temporal frequency and the highest temporal frequency to evoke responses 50% of maximum (TF_{50}).

Fano factor analysis

Response reliability was quantified by calculating the Fano factor from responses to >48 cycles of a drifting grating (100% contrast, 4 Hz, optimal spatial frequency).

$$\text{Fano factor} = \text{variance of spike count/mean spike count}$$

Gratings were presented in blocks of 12 or 16 cycles. For each block, the first 3 cycles were excluded from analysis to avoid onset transients. Fano factors were also calculated using the full response and were not significantly different from those with the first 3 cycles removed. Fano factors were calculated using two different bin sizes, 250 ms (full stimulus cycle) and 16.6 ms (a value reflecting the integration time of postsynaptic cortical neurons; Usrey *et al.* 2000).

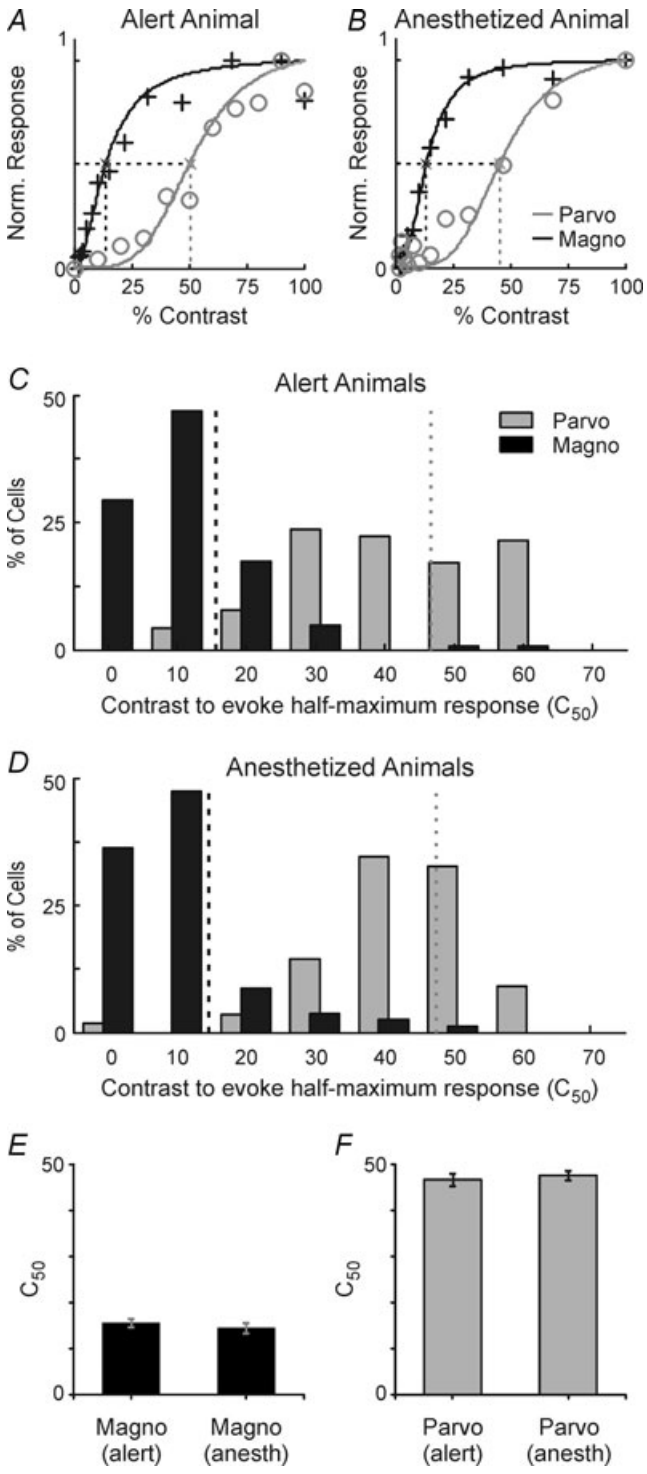

Figure 1. Comparison of contrast response functions from LGN neurons in alert and anaesthetized animals
A and *B*, contrast response functions from individual magnocellular neurons (black traces) and parvocellular neurons (grey traces) in the alert and anaesthetized animal. Data points are fitted to a hyperbolic ratio (Albrecht & Hamilton, 1982). Dashed lines indicate the contrast needed to evoke a response 50% of maximum (C_{50}). *C* and *D*, histograms showing the distribution of C_{50} values for magnocellular and parvocellular neurons in alert animals and anaesthetized animals. Dashed lines indicate the means for each group of neurons. *E* and *F*, comparison of C_{50} values for magnocellular neurons in alert and anaesthetized animals and parvocellular neurons in alert and anaesthetized animals. C_{50} values did not differ significantly for magnocellular neurons or parvocellular neurons in the two conditions.

Statistical analysis

When sample averages (arithmetic mean) are provided, they are followed by the standard error of the mean (± S.E.M.).

Results

We recorded single-unit, extracellular responses from LGN neurons in two alert macaque monkeys ($n = 59$ magnocellular neurons, 49 parvocellular neurons) and 10 macaque monkeys anaesthetized with a combination of sufentanil citrate ($6\,\mu g\,kg^{-1}\,h^{-1}$) and isoflurane (0.4%; $n = 32$ magnocellular neurons, 31 parvocellular neurons).

Contrast response functions

Contrast response functions were generated from neuronal responses to drifting sinusoidal gratings (4 Hz, preferred spatial frequency) that varied in contrast from 0.1 to 100%. Response functions from four representative neurons – a magnocellular and parvocellular neuron in the alert animal and a magnocellular and parvocellular neuron in the anaesthetized animal – are shown in Fig. 1*A* and *B*, respectively. Consistent with previous reports, the magnocellular neurons responded better to low contrast stimuli than the parvocellular neurons (Kaplan & Shapley, 1986). The magnocellular neurons also displayed response saturation to high contrast stimuli whereas the parvocellular neurons continued to increase their responses as contrast increased.

To compare quantitatively the response functions of LGN neurons in alert and anaesthetized animals, we calculated the contrast needed to evoke 50% of each neuron's maximum response (C_{50}). As shown in Fig. 1*C* and *D*, the distributions of C_{50} values for magnocellular and parvocellular neurons were largely non-overlapping for both alert and anaesthetized animals. More importantly, C_{50} values were not significantly different for magnocellular neurons in alert and anaesthetized animals (Fig. 1*E*; $15.7 \pm 0.9\%$ *vs.* $14.6 \pm 1.1\%$, respectively; $P = 0.27$, Wilcoxon's rank-sum test) nor were they significantly different for parvocellular neurons in the two groups of animals (Fig. 1*F*; $46.8 \pm 1.3\%$ *vs.* $47.6 \pm 1.6\%$, respectively; $P = 0.68$, *t* test). Thus, anaesthesia does not have an appreciable influence on the overall shape of contrast response functions in the macaque LGN (Fig. 2*A* and *B*).

Although anaesthesia did not influence the stereotypical shapes of magnocellular and parvocellular contrast response functions, it did influence firing rate for both groups of neurons. To quantify this effect, we measured each neuron's peak firing rate from their contrast response function. As shown in Fig. 2*C* and *D*, peak firing rate was 1.3 times greater, on average, for magnocellular neurons and 2.1 times greater for parvocellular neurons in alert animals compared to anaesthetized animals (magnocellular neurons: alert = 45.4 ± 2.5 spikes s^{-1}, anaesthetized = 34.5 ± 3.6 spikes s^{-1}, $P < 0.01$, Wilcoxon's rank-sum test; parvocellular neurons: alert = 41.8 ± 2.5 spikes s^{-1}, anaesthetized 19.7 ± 2.4 spikes s^{-1}, $P < 0.01$, Wilcoxon's rank-sum test). Because anaesthesia did not affect C_{50} values (described above) or the normalized shape of contrast response functions, the reduction in peak firing rate indicates that anaesthesia acts to scale neuronal firing rate in a divisive fashion over a wide range of contrasts.

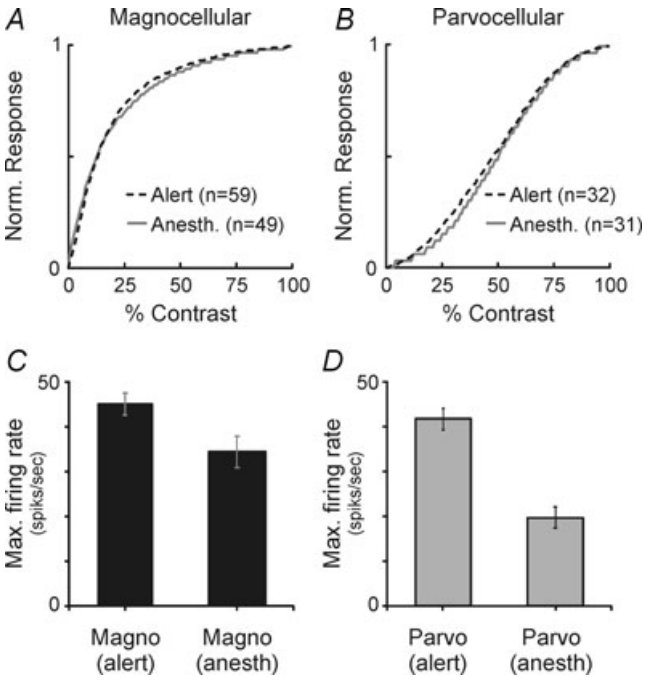

Figure 2. Normalized contrast response functions and maximum firing rates for LGN neurons in alert and anaesthetized animals
A and *B*, average contrast response functions for magnocellular and parvocellular neurons in alert (dashed lines) and anaesthetized animals (continuous lines). *C* and *D*, comparison of maximum-evoked responses for magnocellular and parvocellular neurons in alert and anaesthetized animals. Maximum firing rate determined from each neuron's contrast response function. Firing rates are significantly greater for magnocellular and parvocellular neurons in alert animals compared to anaesthetized animals.

Temporal frequency tuning

Past studies have shown that neurons in the magnocellular layers of the LGN typically follow stimuli drifting at higher temporal frequencies than neurons in the parvocellular layers (Hicks *et al.* 1983; Derrington & Lennie, 1984; Levitt *et al.* 2001; Movshon *et al.* 2005; but see Spear *et al.* 1994; Hawken *et al.* 1996). To compare temporal frequency tuning among magnocellular and parvocellular neurons in the alert and anaesthetized animal, we determined each neuron's preferred temporal frequency (Fig. 3*A* and *B*, arrows) and highest temporal frequency to evoke responses 50% of maximum (TF_{50}; Fig. 4*A* and *B*, crosses). For both magnocellular and parvocellular neurons, preferred temporal frequencies were significantly greater in alert animals compared to anaesthetized animals (Fig. 3*C–F*; magnocellular neurons: alert = 21.3 ± 1.3 Hz, anaesthetized = 10.0 ± 1.3 Hz, $P < 0.01$, Wilcoxon's rank-sum test; parvocellular neurons: alert = 14.9 ± 1.3 Hz, anaesthetized = 6.2 ± 0.4 Hz, $P < 0.01$, Wilcoxon's rank-sum test). Similarly, TF_{50} values were significantly greater in alert animals compared to anaesthetized animals (Fig. 4*C–F*; magnocellular neurons: alert = 45.2 ± 1.2 Hz, anaesthetized = 25.8 ± 2.2 Hz, $P < 0.01$, Wilcoxon's rank-sum test; parvocellular neurons: alert = 32.3 ± 1.9 Hz, anaesthetized = 11.4 ± 0.9 Hz, $P < 0.01$, Wilcoxon's rank-sum test). As somewhat of a surprise, the differences in temporal frequency tuning between alert and anaesthetized animals were so substantial that both the preferred temporal frequency and TF_{50} were greater, on average, for alert parvocellular neurons compared to anaesthetized magnocellular neurons (Fig. 3*E* and *F*).

An examination of peak firing rate using data from each neuron's temporal frequency tuning curve also revealed significantly higher response rates among magnocellular and parvocellular neurons in the alert animal compared to the anaesthetized animal (magnocellular neurons: alert = 50.1 ± 3.8 spikes s^{-1}, anaesthetized = 22.0 ± 2.2 spikes s^{-1}, $P < 0.01$, *t* test; parvocellular neurons: alert = 38.4 ± 2.6 spikes s^{-1}, anaesthetized = 10.7 ± 1.1 spikes s^{-1}; $P < 0.01$, *t* test).

Spatial frequency tuning and surround antagonism

Past studies report wide ranges and overlapping distributions of spatial frequency preferences for magnocellular and parvocellular neurons with an overall trend of parvocellular neurons preferring higher spatial frequencies than magnocellular neurons and a decrease in preferred spatial frequency with eccentricity (Derrington & Lennie, 1984; Spear *et al.* 1994; Usrey & Reid, 2000; Levitt *et al.* 2001). We found similar relationships for magnocellular and parvocellular neurons in alert and anaesthetized animals. To determine whether

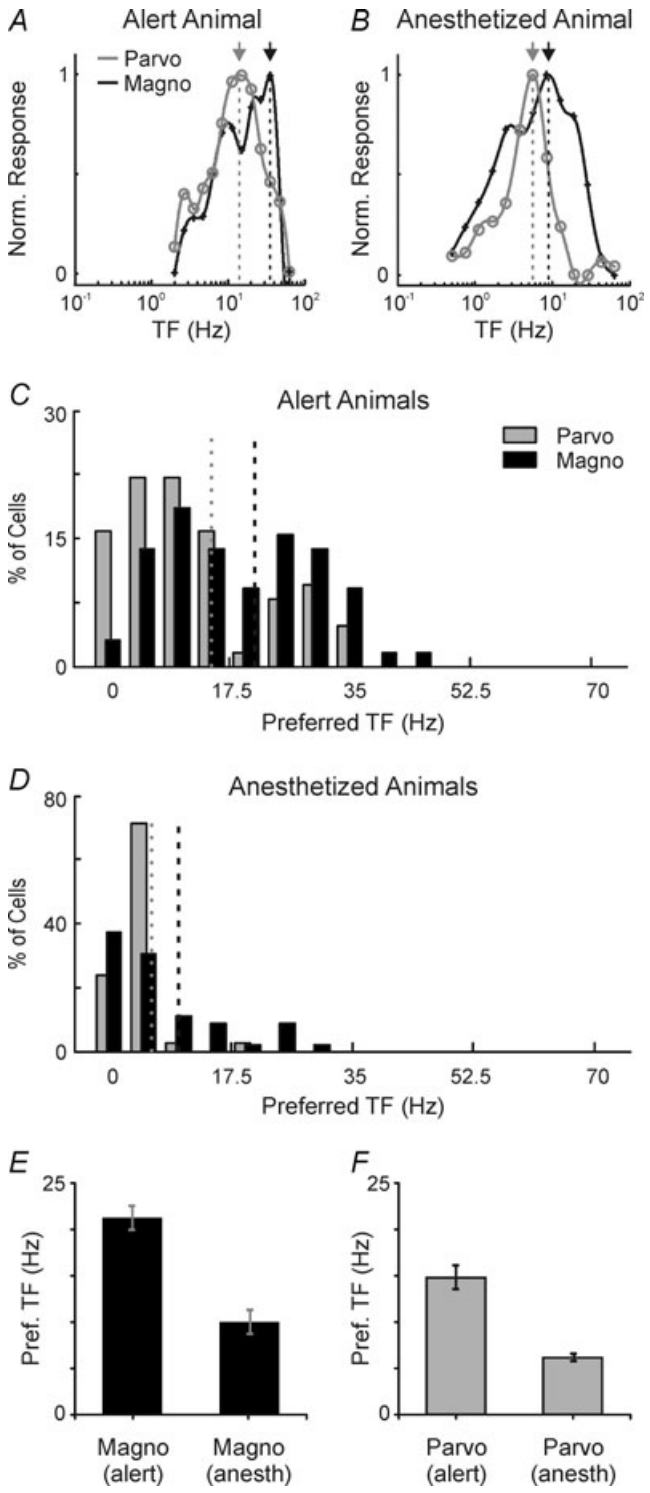

Figure 3. Temporal frequency tuning curves and comparison of preferred temporal frequencies for LGN neurons in alert and anaesthetized animals
A and *B*, temporal frequency tuning curves from individual magnocellular neurons (black traces) and parvocellular neurons (grey traces) in the alert and anaesthetized animal. Data points are interpolated with a cubic spline. Dashed lines indicate each neuron's preferred temporal frequency. *C* and *D*, histograms showing the distribution of preferred temporal frequencies for magnocellular and parvocellular neurons in alert animals (n = 59 magno neurons and 49 parvo neurons) and anaesthetized animals (n = 32 magno neurons and 31 parvo neurons). Dashed lines indicate the means for each group of neurons. *E* and *F*, comparison of preferred temporal frequencies for magnocellular neurons in alert and anaesthetized animals and parvocellular neurons in alert and anaesthetized animals. Preferred temporal frequencies are significantly higher for both magnocellular and parvocellular neurons in alert animals compared to anaesthetized animals.

brain state has an influence on spatial frequency tuning, we identified each neuron's highest spatial frequency to evoke responses 50% of maximum (SF_{50}; Fig. 5*A–D*). While SF_{50} values were not significantly different for parvocellular neurons in the alert and anaesthetized animal (Fig. 5; 2.95 ± 0.17 *vs.* 3.16 ± 0.70 cycles deg^{-1}, respectively; $P = 0.20$, Wilcoxon's rank-sum test), they were significantly higher for magnocellular neurons in the alert animal compared to the anaesthetized animal (Fig. 5*E*; 2.59 ± 0.11 *vs.* 1.65 ± 0.25 cycles deg^{-1}, respectively; $P < 0.01$, Wilcoxon's rank-sum test). To ensure this increase in SF_{50} was not influenced by differences in the distributions of receptive field locations, we repeated this analysis using a matched subset of cells from the alert and anaesthetized animal where cell pairs were randomly selected with the criterion that their receptive field eccentricities were less than 1 deg apart (n = 16 pairs; mean eccentricity: alert = 6.33 deg, anaesthetized = 6.27 deg). Results from this comparison also revealed significantly higher SF_{50} values for magnocellular neurons in the alert animal compared to the anaesthetized animal (2.44 ± 0.17 *vs.* 1.73 ± 0.28; $P < 0.05$, Wilcoxon's rank-sum test).

To evaluate surround antagonism in alert and anaesthetized animals, we compared neuronal responses to gratings of optimal spatial frequency (which modulate the centre, but not the surround) with responses to gratings of low spatial frequency (which modulate the centre and surround antagonistically; Fig. 6*A* and *B*). The strength of surround antagonism was quantified using an antagonism index (see Methods), where values near 1 represent cells with strong surround antagonism and values near 0 represent cells with weak antagonism. As shown in Fig. 6*C* and *D*, index values for magnocellular and parvocellular neurons in alert and anaesthetized animals were broadly distributed and overlapping. Consistent with previous results from the squirrel monkey and owl monkey, parvocellular neurons displayed slightly greater surround antagonism than magnocellular neurons (Usrey & Reid, 2000). More importantly, there was not a significance difference between antagonism index values among magnocellular neurons in the alert and anaesthetized animal (Fig. 6*E*; 0.44 ± 0.33 *vs.* 0.52 ± 0.06, respectively; $P = 0.25$, rank-sum test) or between parvocellular neurons in the alert and anaesthetized

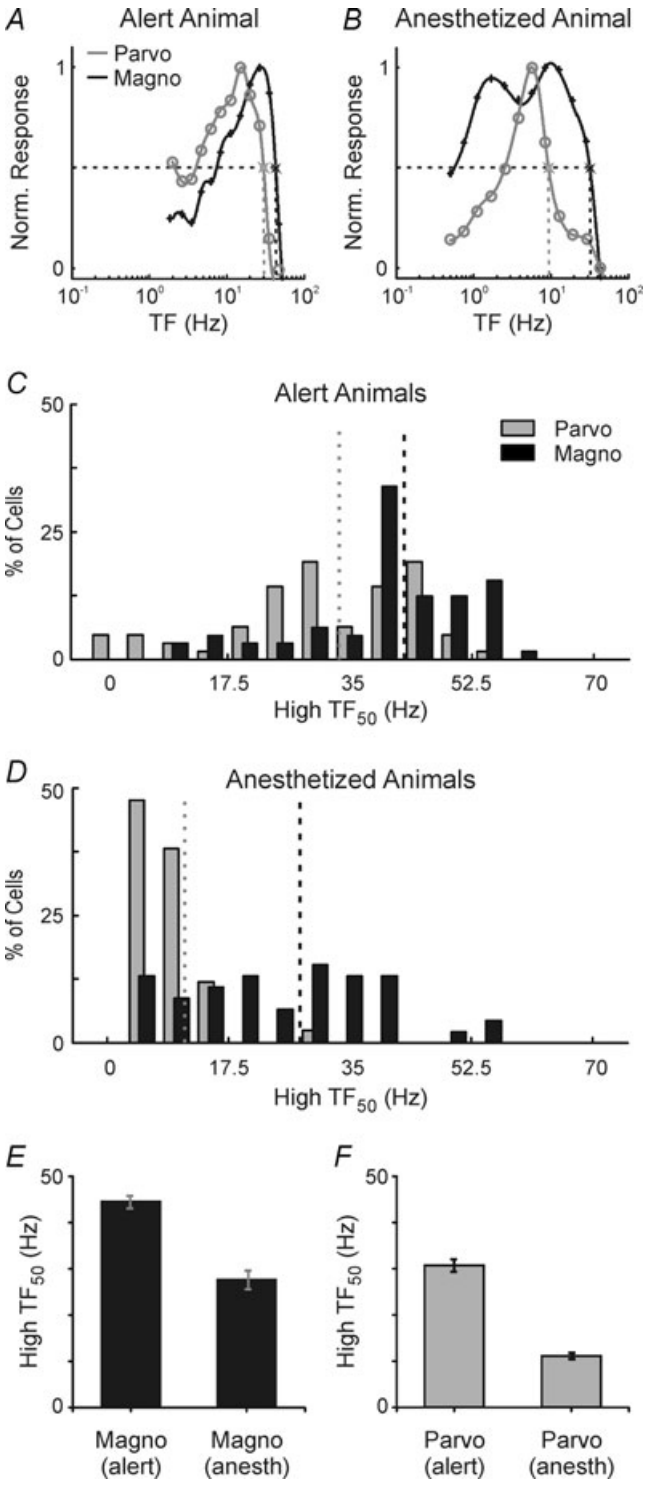

Figure 4. Comparison of high temporal frequency cutoff for LGN neurons in alert and anaesthetized animals
A and *B*, temporal frequency tuning curves from individual magnocellular neurons (black traces) and parvocellular neurons (grey traces) in the alert and anaesthetized animal. Data points are interpolated with a cubic spline. Dashed lines indicate the highest temporal frequency that will evoke a response 50% of maximum (TF_{50}). *C* and *D*, histograms showing the distribution of TF_{50} values for magnocellular and parvocellular neurons in alert animals ($n = 59$ magno neurons and 49 parvo neurons) and anaesthetized animals ($n = 32$ magno neurons and 31 parvo neurons). Dashed lines indicate the means for each group of neurons. *E* and *F*, comparison of TF_{50} values from magnocellular neurons in alert and anaesthetized animals and parvocellular neurons in alert and anaesthetized animals. TF_{50} values are significantly higher for both magnocellular and parvocellular neurons in alert animals compared to anaesthetized animals.

animal (Fig. 6*F*; 0.64 ± 0.03 *vs.* 0.52 ± 0.07, respectively; $P = 0.33$, rank-sum test).

Response reliability

To address the question of whether brain state affects the reliability of LGN responses, we calculated the Fano factor (response variance/mean response) for LGN neurons excited with a drifting 4 Hz sinusoidal grating of preferred spatial frequency and 100% contrast (Methods). Similar to previous descriptions of LGN responses in the anaesthetized cat and primate, both magnocellular and parvocellular LGN neurons in the alert and anaesthetized macaque monkey displayed sub-Poisson statistics with Fano factor values less than 1.0 (Fig. 7; Kara *et al.* 2000; Andolina *et al.* 2007; Victor *et al.* 2007). Although Fano factor values were similar (and lowest) among the four groups of neurons when this analysis was performed using a bin size corresponding to a full cycle of the sinusoidal stimulus (250 ms; Fig. 7*A*), some differences were apparent with smaller bin sizes. In particular, with a relatively small bin size (16.6 ms), Fano factor values were significantly less for magnocellular neurons than for parvocellular neurons (Fig. 7*B*, $P < 0.01$). This result indicates that magnocellular neurons display greater response precision and reliability during time epochs relevant for the postsynaptic summation of LGN inputs to cortex (Usrey *et al.* 2000). However, even with a bin size of 16.6 ms, there was little effect of brain state on response reliability.

Bursting and spontaneous activity

Similar to other thalamic neurons, LGN neurons produce spikes that can be classified as burst spikes or tonic spikes. Whether or not an LGN neuron generates burst or tonic spikes depends on the neuron's membrane potential history and the activation state of the T-type Ca^{2+} channel (Jahnsen & Llinás, 1984*a*,*b*; Zhou *et al.* 1997; Destexhe *et al.* 1998). Namely, if the cell's resting membrane potential is relatively depolarized, then T-type Ca^{2+} channels are in an inactivated state and suprathreshold inputs evoke tonic Na^{+} spikes. In contrast, if the cell's resting potential is more hyperpolarized, then T-type channels become de-inactivated and suprathreshold inputs evoke

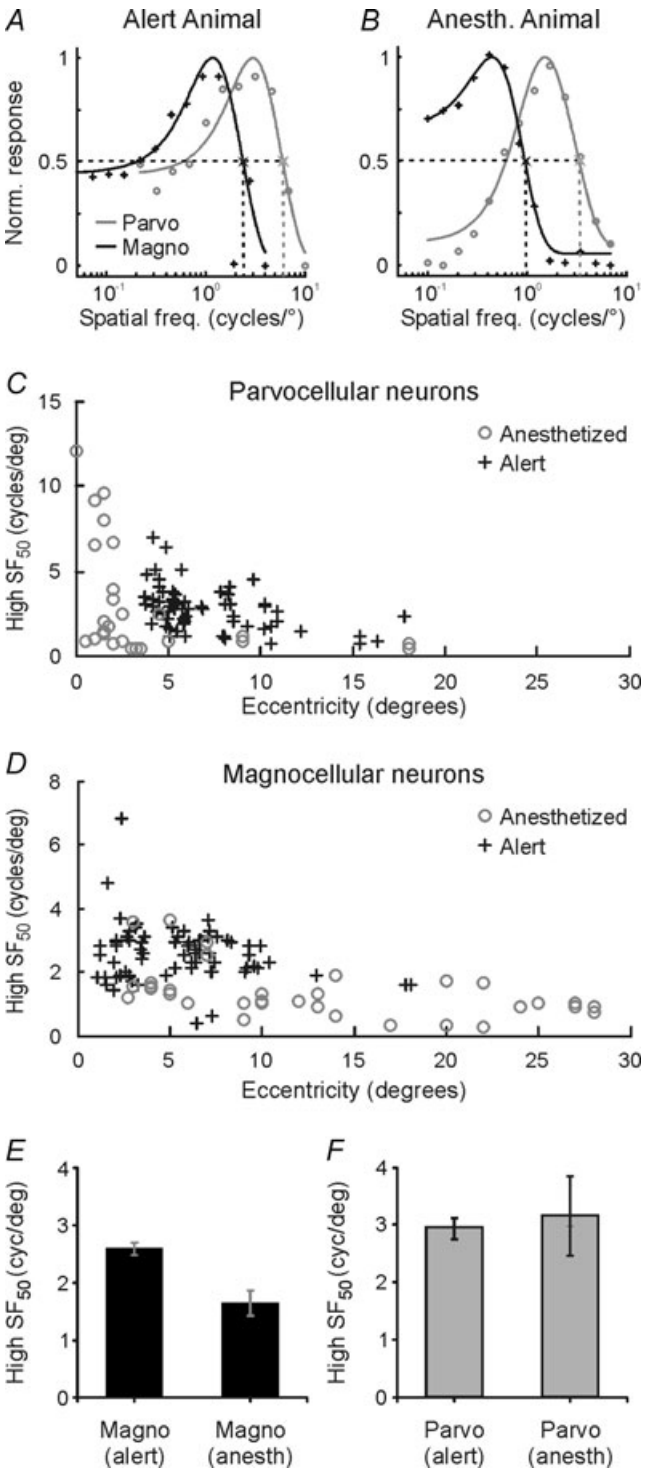

Figure 5. Comparison of high spatial frequency cutoff for LGN neurons in alert and anaesthetized animals
A and *B*, spatial frequency tuning curves from individual magnocellular neurons (black traces) and parvocellular neurons (grey traces) in the alert and anaesthetized animal. Data points fitted with a difference of Gaussians (DOG) equation (see Methods). Dashed lines indicate the highest spatial frequency that will evoke a response 50% of maximum (SF_{50}). *C* and *D*, scatterplots showing the distribution of High SF_{50} values for magnocellular and parvocellular neurons in alert and anaesthetized animals as a function of eccentricity. *E* and *F*, comparison of SF_{50} values from magnocellular neurons in alert and anaesthetized animals and parvocellular neurons in alert and anaesthetized animals. SF_{50} values are significantly higher for magnocellular neurons in alert animals compared to anaesthetized animals. SF_{50} values are not significantly different for parvocellular neurons in alert and anaesthetized animals.

a low-threshold Ca^{2+} current that triggers a burst of Na^{+} spikes. Because T-type Ca^{2+} channels need to be hyperpolarized for >50 ms to become de-inactivated, this criterion (>50 ms of non-spiking, followed by 2 or more spikes with interspike intervals <4 ms) has been applied with success to identify low-threshold bursts with extracellular electrodes *in vivo* (Lo *et al.* 1991; Lu *et al.* 1992).

Similar to results from previous studies (Weyand *et al.* 2001; Bezdudnaya *et al.* 2006; Ruiz *et al.* 2006), there were significantly fewer bursts in the alert monkey compared to the anaesthetized monkey (Fig. 8*A* and *B*; $P < 0.01$, ANOVA). Indeed, for both magnocellular and parvocellular neurons, anaesthesia increased the percentage of spikes classified as burst spikes by ~3 times. These findings indirectly indicate that LGN neurons in the macaque monkey are more hyperpolarized under anaesthesia, a view supported by the findings that anaesthesia decreased both the spontaneous activity of neurons (Fig. 8*C* and *D*; $P < 0.01$; ANOVA) and the maximum evoked activity of neurons (Fig. 2).

Discussion

From the earliest days of microelectrode recordings, researchers have recognized that sensory responses differ between alert and anaesthetized animals. In particular, early studies indicated that single-unit responses in the alert animal are more robust and subject to influences from behaviour and attention (Hubel *et al.* 1959; Poggio & Mountcastle, 1963). For these reasons, along with ease of training and similarities with human vision, the alert macaque monkey is widely used in studies investigating visual processing, particularly in the cerebral cortex. Despite our increased understanding of visual responses in the cortex of alert animals, our understanding of the physiology of visual inputs to the cortex comes primarily from recordings in anaesthetized animals. The goal of this study was to assess visual responses from neurons in the LGN of alert monkeys and compare these responses to those from anaesthetized animals.

Results from numerous studies examining LGN responses in anaesthetized monkeys demonstrate significant differences between magnocellular and parvocellular neurons. In particular, magnocellular neurons have greater sensitivity to low contrast stimuli

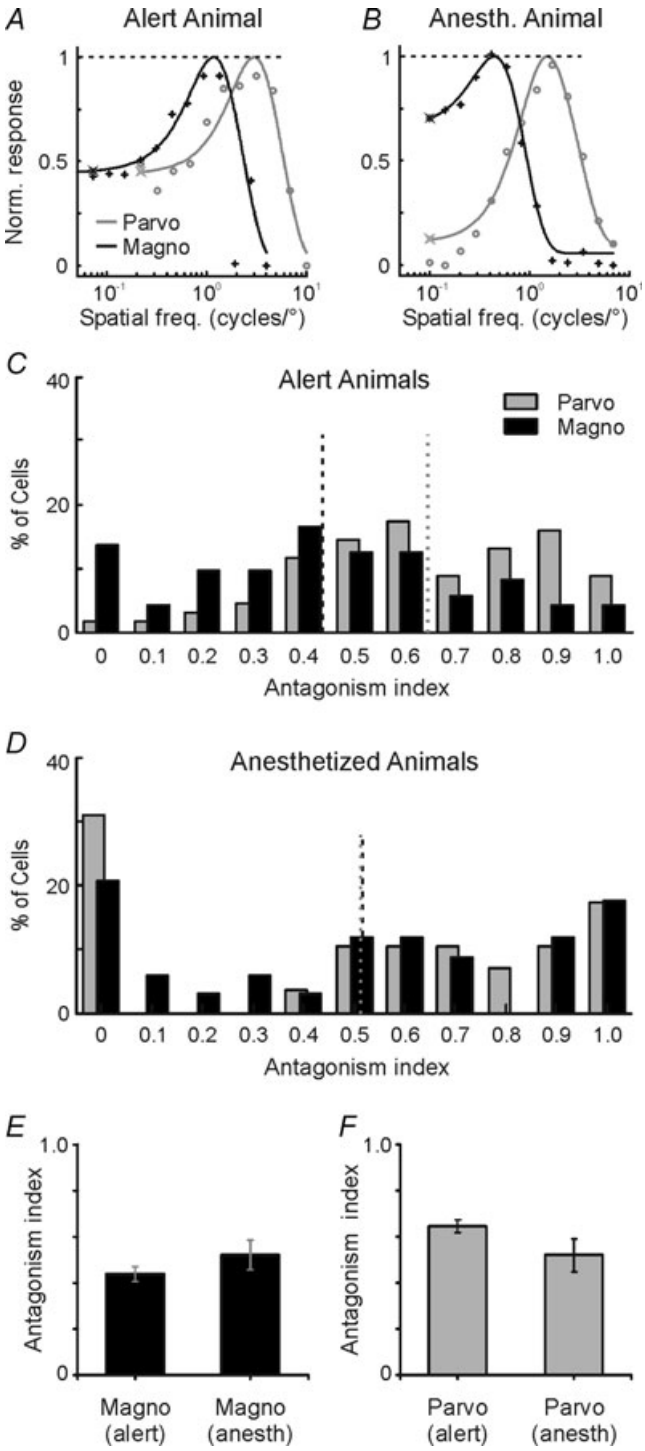

Figure 6. Surround antagonism in the LGN of alert and anaesthetized animals
A and *B*, spatial frequency tuning curves from individual magnocellular neurons (black traces) and parvocellular neurons (grey traces) in the alert and anaesthetized animal. Data points are fitted with a difference of Gaussians equation. Dashed lines represent responses to preferred spatial frequency; stars represent responses to lowest spatial frequency examined. *C* and *D*, histograms showing the distribution of antagonism index values (see Methods) for magnocellular and parvocellular neurons in alert animals (n = 73 magno neurons and 69 parvo neurons) and anaesthetized animals (n = 34 magno neurons and 39 parvo neurons). Dashed lines indicate the means for each group of neurons. *E* and *F*, comparison of antagonism index values from magnocellular neurons in alert and anaesthetized animals and parvocellular neurons in alert and anaesthetized animals. Index values are not significantly different for magnocellular or parvocellular neurons in alert and anaesthetized animals.

and follow stimuli at higher temporal frequencies than parvocellular neurons (Kaplan & Shapley, 1982, 1986; Derrington & Lennie, 1984; Norton *et al.* 1988; Benardete *et al.* 1992; O'Keefe *et al.* 1998; Solomon *et al.* 1999; Usrey & Reid, 2000; Levitt *et al.* 2001; Movshon *et al.* 2005; but see Spear *et al.* 1994; Hawken *et al.* 1996). Our results from the alert animal show a similar relationship between magnocellular and parvocellular neurons. However, a closer examination of neuronal response functions reveals some significant differences between alert and anaesthetized animals. Notably, neuronal firing rates were significantly higher in alert animals compared to anaesthetized animals. This increase in firing rate was not accompanied by a change in the overall shape of magnocellular and parvocellular contrast responses functions; however, it was accompanied by a significant increase in the ability of magnocellular and parvocellular neurons to follow stimuli at high temporal frequencies and by an increase in the ability of magnocellular neurons to follow high spatial frequencies. In the sections below, we compare our results to those of past studies and consider their functional implications.

Comparing responses in alert and anaesthetized animals

Despite an overall increase in the firing rate of magnocellular and parvocellular neurons in alert animals, contrast response functions from these neurons appeared similar in shape to those from anaesthetized animals. Similar results have been reported for awake rabbits as they shift between alert and non-alert states (Cano *et al.* 2006). These finding indicates that contrast response functions are scaled multiplicatively in alert and attentive animals. Consistent with this view, a recent modelling study that included data from Sanchez-Vives *et al.* (2000) demonstrates that alterations in the membrane potential of cortical neurons results in a multiplicative/divisive scaling of their contrast response functions (Murphy & Miller, 2003). Since many anaesthetic agents can influence the membrane potential of thalamic neurons (Ries & Puil, 1999), these three sets of results are consistent and complementary.

Our results demonstrate that magnocellular and parvocellular neurons in alert animals prefer stimuli

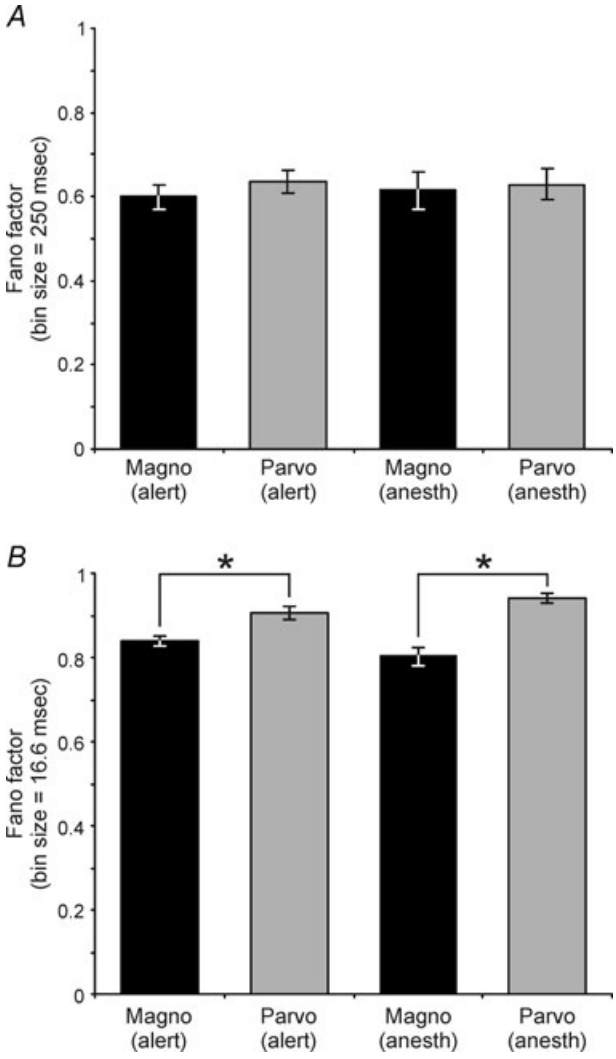

Figure 7. Response reliability in the LGN of alert and anaesthetized animals
A and *B*, Fano factor values (response variance/mean response) for magnocellular and parvocellular neurons in the alert and anaesthetized animal. *A*, mean Fano factor values for the 4 categories of LGN neurons – magnocellular and parvocellular neurons in the alert animal (0.60 ± 0.03 and 0.64 ± 0.03, respectively), and magnocellular and parvocellular neurons in the anaesthetized animal (0.61 ± 0.04 and 0.63 ± 0.04, respectively) – calculated using a bin size of 250 ms. With this bin size, there was no significant difference in the Fano factor of magnocellular and parvocellular neurons or in the Fano factor of neurons in the anaesthetized and alert animal ($P = 0.54$ and 0.92, respectively). *B*, mean Fano factor values for the 4 categories of LGN neurons – magnocellular and parvocellular neurons in the alert animal (0.84 ± 0.01 and 0.91 ± 0.02, respectively), and magnocellular and parvocellular neurons in the anaesthetized animal (0.80 ± 0.02 and 0.94 ± 0.01, respectively) – calculated using a bin size of 16.6 ms. With this bin size, there was a significant difference in the Fano factor of magnocellular and parvocellular neurons ($P < 0.01$), but not in the Fano factor of neurons in the alert and anaesthetized animal ($P = 0.96$).

drifting at higher temporal frequencies and have higher cutoff frequencies than in animals anaesthetized with a combination of sufentanil and isoflurane. Sufentanil is a powerful opiod analgesic with a relative potency 500–1000 times that of morphine and, when given at sufficient doses, can produce surgical levels of anaesthesia (Helmers *et al.* 1989; Miller *et al.* 2009). Sufentanil binds to opiod (G-protein coupled) receptors and acts, in part, on GABAergic transmission. Because sufentanil has less depressing actions on cortical activity than other anaesthetic agents, it has become a preferred anaesthetic agent for neurophysiological recordings in primates. Although the amount of isoflurane (0.4%) used in this study would not be sufficient for anaesthesia in the absence of sufentanil, it is important to be aware that most

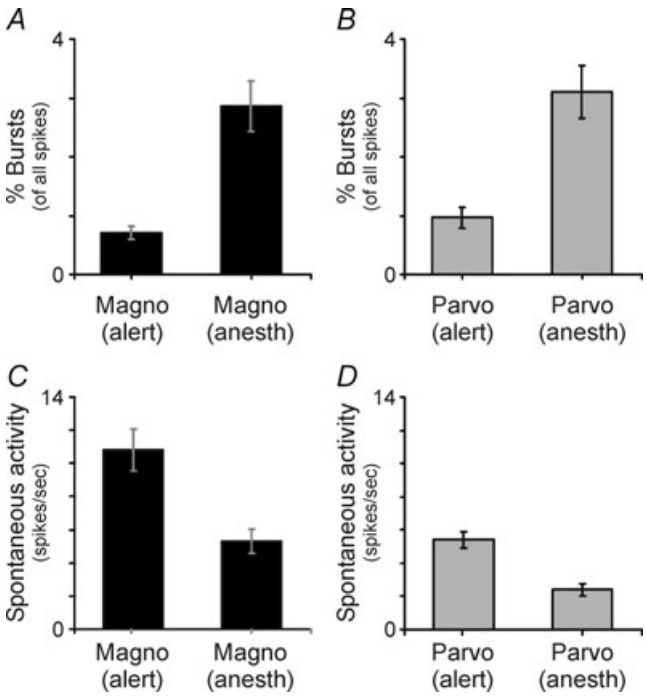

Figure 8. Burst activity and spontaneous activity in the LGN of alert and anaesthetized animals
A and *B*, histograms showing the percentage of spikes classified as burst spikes for magnocellular and parvocellular neurons in the alert ($n = 59$ magno neurons and 49 parvo neurons) and anaesthetized animal ($n = 32$ magno neurons and 31 parvo neurons). For magnocellular neurons in the alert and anaesthetized animal, burst spikes comprised 0.7 ± 0.1% and 2.8 ± 0.4% of all spikes, respectively ($P < 0.01$; ANOVA). For parvocellular neurons in the alert and anaesthetized animal, burst spikes comprised 1.0 ± 0.2% and 3.1 ± 0.5% of all spikes, respectively ($P < 0.01$; ANOVA). *C* and *D*, histograms showing spontaneous activity levels (spikes s^{-1}) for magnocellular and parvocellular neurons in the alert and anaesthetized animal. For magnocellular neurons in the alert and anaesthetized animal, spontaneous activity levels were 10.8 ± 1.3 spikes s^{-1} and 5.3 ± 0.4 spikes s^{-1}, respectively ($P < 0.01$; ANOVA). For parvocellular neurons in the alert and anaesthetized animal, spontaneous activity levels were 5.4 ± 0.5 spikes s^{-1} and 2.4 ± 0.4 spikes s^{-1}, respectively ($P < 0.01$; ANOVA).

studies investigating visual processing in the macaque monkey avoid isoflurane due to its suppressive influence on cortical responses. With this in mind, it is worth noting that the preferred temporal frequencies and/or high cutoff frequencies reported in past studies using either sufentanil, fentanil, or nembutal exclusively for anaesthesia are typically less than those reported here for alert animals (Derrington & Lennie, 1984; Spear *et al.* 1994; Hawken *et al.* 1996; Levitt *et al.* 2001; Movshon *et al.* 2005; but see Hicks *et al.* 1983). Along these lines, recent results indicate that the influence of brain state on temporal frequency tuning extends beyond effects mediated by anaesthesia, as LGN neurons in awake rabbits follow higher temporal frequencies when animals are in an attentive state compared to a non-attentive state (Bezdudnaya *et al.* 2006). Likewise, spatial attention has been shown to modulate activity levels in the LGN of macaque monkeys and humans (O'Connor *et al.* 2002; Casagrande *et al.* 2005; McAlonan *et al.* 2008).

Compared to LGN neurons in the alert animal, LGN neurons in the anaesthetized animal had lower levels of spontaneous activity, lower peak firing rates and increased burstiness. Each of these differences is consistent with the view that anaesthesia increased the hyperpolarization of neurons. While this hyperpolarization affected the visual responsiveness of LGN neurons, it did not affect the relative strength of the centre and surround subunits in the classical receptive field (Fig. 6). Along these lines, the relative strength of the extraclassical surround has also been shown to be similar for LGN neurons in alert and anaesthetized animals (Alitto & Usrey, 2008). Increased hyperpolarization with anaesthesia could result from decreased excitation, increased inhibition, or both. It is therefore interesting to note that layer 6 corticogeniculate neurons, a major source of glutamateric synapses in the LGN (Guillery, 1969), are less responsive in anaesthetized animals (Briggs & Usrey, 2007, 2009). Perhaps more importantly, local interneurons providing GABAergic input to LGN relay cells have receptive fields with a centre–surround organization that is very similar to that of their target cells (Wang *et al.* 2007). Because these interneurons provide a 'pull' that compliments the 'push' supplied by the retina, changes in the strength of their inhibition should affect the centre and surround subunits similarly – a prediction supported by our finding that surround antagonism is similar for LGN neurons in the alert and anaesthetized animal.

Functional implications

Throughout this study, parvocellular neurons typically displayed greater differences in their response properties between alert and anaesthetized animals than magnocellular neurons. This was particularly noteworthy for measures of maximum firing rate and high temporal frequency cutoff. While the reasons for this differential influence of anaesthesia are unclear, two likely possibilities include (1) a cell size-dependent or membrane-specific influence of anaesthesia (Urban, 2008), whereby small cells are more affected by anaesthesia than large cells (mean cross-sectional area of parvocellular neurons is ∼40% less than that of magnocellular neurons; Weber *et al.* 2000; see also Montero & Zempel, 1985; Ahmad & Spear, 1993), and (2) differential effects of anaesthesia on the specific circuits and/or balance of excitation and inhibition that underlie magnocellular and parvocellular responses.

Across the four categories of neurons examined here, parvocellular and magnocellular neurons in the anaesthetized animal and parvocellular and magnocellular neurons in the alert animal, there was a positive relationship between maximum evoked firing rate and high temporal-frequency cutoff or TF_{50}. Specifically, parvocellular neurons in the anaesthetized animal had the lowest mean firing rate and lowest mean TF_{50} (10.7 spikes s^{-1}; 11.4 Hz), followed by magnocellular neurons in the anaesthetized animal (22.0 spikes s^{-1}; 25.8 Hz), parvocellular neurons in the alert animal (38.4 spikes s^{-1}; 32.3 Hz) and, lastly, magnocellular neurons in the alert animal (50.1 spikes s^{-1}; 45.2 Hz). This finding suggests that mechanisms governing the firing rate of a neuron (e.g. membrane potential and/or intrinsic conductances) may also provide an upper bound or constraint on the temporal frequencies a neuron can follow. Consistent with this view, results from two species of New World monkeys reveal a similar relationship between firing rate and temporal frequency tuning, whereby LGN neurons in the diurnal squirrel monkey, which have higher maximum firing rates, follow higher temporal frequencies than neurons in the nocturnal owl monkey, which have lower maximum firing rates (Usrey & Reid, 2000). Given the relationship between firing rate and temporal frequency tuning, it would be interesting to know whether inputs to the LGN that serve to depolarize neurons, such as histamine and acetylcholine, can adjust the sensitivity of LGN neurons to stimuli presented at different temporal frequencies (Zhu & Uhlrich, 1997; Uhlrich *et al.* 2002).

Concluding remarks

This study provides a quantitative analysis of the response properties of LGN neurons in the alert macaque monkey and compares these values to those in monkeys under anaesthesia. Our results demonstrate that LGN neurons in the alert and anaesthetized animal do not differ in terms of the relative strength of their centre and surround subunits, the shape of their contrast response functions or their response reliability. In contrast, magnocellular and parvocellular neurons in the alert animal have increased

peak and spontaneous levels of activity, decreased burstiness, and a greater ability to follow stimuli at high temporal frequencies. Magnocellular neurons in the alert animal also follow stimuli with higher spatial frequencies. Thus, a greater range of spatiotemporal features in the visual scene are conveyed to the cortex in alert animals than was previously appreciated from recordings in anaesthetized animals. In addition, the increased firing rate of LGN neurons in the alert animal is likely to underlie a greater functional coupling between the LGN and visual cortex, as firing rate and interspike interval are known to influence the dynamics of synaptic communication between pre- and postsynaptic neurons in the two structures (Usrey *et al.* 2000).

References

Ahmad A & Spear PD (1993). Effects of aging on the size, density, and number of rhesus monkey lateral geniculate neurons. *J Comp Neurol* **334**, 631–643.

Albrecht DG & Hamilton DB (1982). Striate cortex of monkey and cat: contrast response function. *J Neurophysiol* **48**, 217–237.

Alitto HJ & Usrey WM (2008). Origin and dynamics of extraclassical suppression in the lateral geniculate nucleus of the macaque monkey. *Neuron* **57**, 135–146.

Andolina IM, Jones HE, Wang W & Sillito AM (2007). Corticothalamic feedback enhances stimulus response precision in the visual system. *Proc Natl Acad Sci U S A* **104**, 1685–1690.

Benardete EA, Kaplan E & Knight BW (1992). Contrast gain control in the primate retina: P cells are not X-like, some M cells are. *Visual Neurosci* **8**, 483–486.

Bezdudnaya T, Cano M, Bereshpolova Y, Stoelzel CR, Alonso JM & Swadlow HA (2006). Thalamic burst mode and inattention in the awake LGNd. *Neuron* **49**, 421–432.

Briggs F & Usrey WM (2007). A fast, reciprocal pathway between the lateral geniculate nucleus and visual cortex in the macaque monkey. *J Neurosci* **27**, 5431–5466.

Briggs F & Usrey WM (2009). Parallel processing in the corticogeniculate pathway of the macaque monkey. *Neuron* **62**, 135–146.

Campagna JA, Miller KW & Forman SA (2003). Mechanisms of actions of inhaled anesthetics. *N Engl J Med* **348**, 2110–2124.

Cano M, Bezdudnaya T, Swadlow HA &Alonso JM (2006). Brain state and contrast sensitivity in the awake visual thalamus. *Nat Neurosci* **9**, 1240–1242.

Casagrande VA, Sary G, Royal D & Ruiz O (2005). On the impact of attention and motor planning on the lateral geniculate nucleus. *Prog Brain Res* **149**, 11–29.

Derrington AM, Krauskopf J & Lennie P (1984). Chromatic mechanisms in lateral geniculate nucleus of macaque. *J Physiol* **357**, 241–265.

Derrington AM & Lennie P (1984). Spatial and temporal contrast sensitivities of neurones in lateral geniculate nucleus of macaque. *J Physiol* **357,** 219–240.

Destexhe A, Neubig M, Ulrich D & Huguenard J (1998). Dendritic low-threshold calcium currents in thalamic relay cells. *J Neurosci* **18**, 3574–3588.

Dilger JP (2002). The effects of general anesthesia on ligand-gated ion channels. *Br J Anesth* **89**, 41–51.

Drummond GB (2009). Reporting ethical matters in *The Journal of Physiology*: standards and advice. *J Physiol* **587**, 713–719.

Evers AS & Crowder CM (2005). Cellular and molecular mechanisms of anesthesia. In *Clinical Anesthesia*, ed. Barash PG, Cullen BF & Stoelting RK, pp. 111–132. Lippincott Williams & Wilkins, Philadelphia.

Guillery RW (1969). A quantitative study of synaptic interconnections in the dorsal lateral geniculate nucleus of the cat. *Z Zellforsch* **96**, 39–48.

Hawken MJ, Shapley RM & Grosof DH (1996). Temporal-frequency selectivity in monkey visual cortex. *Visual Neurosci* **13**, 477–492.

Helmers JH, Van Leeuwen L & Zuurmond W (1989). A sufentanil dosage study in general surgery. *Anaesthesist* **38**, 397–400.

Hicks TP, Lee BB & Vidyasagar TR (1983). The response of cells in macaque lateral geniculate nucleus to sinusoidal gratings. *J Physiol* **337,** 183–200.

Hubel DH, Henson CO, Rupert A & Galambos R (1959). Attention units in the auditory cortex. *Science* **129**, 1279–1280.

Jahnsen H & Llinás R (1984*a*). Electrophysiological properties of guinea-pig thalamic neurones: An in vitro study. *J Physiol* **349**, 205–226.

Jahnsen H & Llinás R (1984*b*). Ionic basis for the electroresponseiveness and oscillatory properties of guinea-pig thalamic neurones *in vitro*. *J Physiol* **349**, 227–247.

Kaplan E & Shapley RM (1982). X and Y cells in the lateral geniculate nucleus of macaque monkeys. *J Physiol* **330**, 125–143.

Kaplan E & Shapley RM (1986). The primate retina contains two types of ganglion cells, with high and low contrast sensitivity. *Proc Natl Acad Sci U S A* **83**, 2755–2757.

Kara P, Reinagel P & Reid RC (2000). Low response variability in simultaneously recorded retinal, thalamic, and cortical neurons. *Neuron* **27**, 635–646.

Levitt JB, Schumer RA, Sherman SM, Spear PD & Movshon JA (2001). Visual response properties of neurons in the LGN of normally reared and visually deprived macaque monkeys. *J Neurophysiol* **85**, 2111–2129.

Lo FS, Lu SM & Sherman SM (1991). Intracellular and extracellular in vivo recordings of different response modes for relay cells of the cat's lateral geniculate nucleus. *Exp Brain Res* **83**, 317–328.

Lu SM, Guido W & Sherman SM (1992). Effects of membrane voltage on receptive field properties of lateral geniculate neurons in the cat: contributions of the low-threshold Ca^{2+} conductance. *J Neurophysiol* **68**, 1285–1298.

McAlonan K, Cavanaugh J &Wurtz RH (2008). Guarding the gateway to cortex with attention in visual thalamus. *Nature* **456**, 391–394.

Miller RD, Eriksson LI, Fleisher LA Wiener-Kronish JP & Young WL (2009). *Miller's Anesthesia*, 7th edn. Churchill Livingstone, Amsterdam.

Montero VM & Zempel J (1985). Evidence for two types of GABA-containing interneurons in the A-laminae of the cat lateral geniculate nucleus: a double-label HRP and GABA-immunocytochemical study. *Exp Brain Res* **60**, 603–609.

Movshon JA, Kiorpes L, Hawken MJ & Cavanaugh JR (2005). Functional maturation of the macaque's lateral geniculate nucleus. *J Neurosci* **25**, 2712–2722.

Murphy BK & Miller KD (2003). Multiplicative gain changes are induced by excitation or inhibition alone. *J Neurosci* **23**, 10040–10051.

Norton TT, Casagrande VA, Irvin GE, Sesma MA & Petry HM (1988). Contrast-sensitivity functions of W-, X-, and Y-like relay cells in the lateral geniculate nucleus of bush baby, *Galago crassicaudatus*. *J Neurophysiol* **59**, 1639–1656.

O'Connor DH, Fukui MM, Pinsk MA & Kastner S (2002). Attention modulates responses in the human lateral geniculate nucleus. *Nat Neurosci* **5**, 1203–1209.

O'Keefe LP, Levitt JB, Kiper DC, Shapley RM & Movshon JA (1998). Functional organization of owl monkey lateral geniculate nucleus and visual cortex. *J Neurophysiol* **80**, 594–609.

Paddleford RR (1999). *Manual of Small Animal Anesthesia*. W.B. Saunders and Co, Philadelphia, PA.

Poggio GF & Mountcastle VB (1963). The functional properties of ventrobasal thalamic neurons studied in unanesthetized monkeys. *J Neurophysiol* **26**, 775–806.

Ries CR & Puil E (1999). Ionic mechanism of isoflurane's actions on thalamocortical neurons. *J Neurophysiol* **81**, 1802–1809.

Rudolph U & Antkowiak B (2004). Molecular and neuronal substrates for general anaesthetics. *Nat Rev Neurosci* **5**, 709–720.

Ruiz O, Royal D, Sáry G, Chen X, Schall JD, Casagrande VA (2006). Low-threshold Ca^{2+}-associated bursts are rare events in the LGN of the awake behaving monkey. *J Neurophysiol* **95**, 3401–3413.

Sanchez-Vives MV, Nowak LG & McCormick DA (2000). Membrane mechanisms underlying contrast adaptation in cat area 17 in vivo. *J Neurosci* **20**, 4267–4285.

Solomon SG, White AJ & Martin PR (1999). Temporal contrast sensitivity in the lateral geniculate nucleus of a New World monkey, the marmoset *Callithrix jacchus*. *J Physiol* **517**, 907–917.

Spear PD, Moore RJ, Kim CB, Xue JT & Tumosa N (1994). Effects of aging on the primate visual system: spatial and temporal processing by lateral geniculate neurons in young adult and old rhesus monkeys. *J Neurophysiol* **72**, 402–420.

Uhlrich DJ, Manning KA & Xue JT (2002). Effects of activation of the histaminergic tuberomammillary nucleus on visual responses of neurons in the dorsal lateral geniculate nucleus. *J Neurosci* **22**, 1098–1107.

Urban BW (2008). The site of anesthetic action. In *Handbook of Experimental Pharmacology*, p. 182. Springer-Verlag, Berlin.

Usrey WM & Reid RC (2000). Visual physiology of the lateral geniculate nucleus in two new world monkeys: *Saimiri sciureus* and *Aotus trivirgatis*. *J Physiol* **523**, 755–769.

Usrey WM, Alonso J-M & Reid RC (2000). Synaptic interactions between thalamic inputs to simple cells in cat visual cortex. *J Neurosci* **20**, 5461–5467.

Victor JD, Blessing EM, Forte JD, Buzas P & Martin PR (2007). Response variability of marmoset parvocellular neurons. *J Physiol* **579**, 29–51.

Wang X, Wei Y, Vaingankar V, Wang Q, Koepsell K, Sommer FT & Hirsch JA (2007). Feedforward excitation and inhibition evoke dual modes of firing in the cat's visual thalamus during naturalistic viewing. *Neuron* **55**, 465–478.

Weber AJ, Chen H, Hubbard WC & Kaufman PL (2000). Experimental glaucoma and cell size, density, and number in the primate lateral geniculate nucleus. *Invest Ophthalmol Vis Sci* **41**, 1370–1379.

Weyand TG, Boudreaux M & Guido W (2001). Burst and tonic response modes in thalamic neurons during sleep and wakefulness. *J Neurophysiol* **85**, 1107–1118.

Zhu JJ & Uhlrich DJ (1997). Nicotinic receptor-mediated responses in relay cells and interneurons in the rat lateral geniculate nucleus. *Neuroscience* **80**, 191–202.

Zhou Q, Godwin DW, O'Malley DM & Adams PR (1997). Visualization of calcium influx through channels that shape the burst and tonic firing modes of thalamic relay cells. *J Neurophysiol* **77**, 2816–2825.

Author contributions

This work was conducted in the laboratory of W.M.U. at the University of California, Davis. H.J.A. and W.M.U. provided conception and design of the experiments, performed data collection, analysis and interpretation of the data, and wrote the article. B.D.M. and D.L.R. performed data collection and interpretation of the data.

Acknowledgements

This work was supported by NIH grants EY13588, EY12576, NSF grant 0727115 and the McKnight Foundation. Kelly Henning, Katie Neverkovec and Daniel Sperka provided expert technical assistance.

Authors' present addresses

H. J. Alitto and B. D. Moore: Helen Wills Neuroscience Institute, University of California – Berkeley, Berkeley, CA 94720, USA.
H. J. Alitto: Howard Hughes Medical Institute, University of California – Berkeley, Berkeley, CA 94720, USA.
D. L. Rathbun: Centre for Integrative Neuroscience, University of Tuebingen, Tuebingen, Germany.